ISSN 1063-7826, Semiconductors, 2018, Vol. 52, No. 6, pp. 789–796. © Pleiades Publishing, Ltd., 2018.
Original Russian Text © T.V. Malin, D.S. Milakhin, V.G. Mansurov, Yu.G. Galitsyn, A.S. Kozhuhov, V.V. Ratnikov, A.N. Smirnov, V.Yu. Davydov, K.S. Zhuravlev, 2018, published in Fizika i Tekhnika Poluprovodnikov, 2018, Vol. 52, No. 6, pp. 643–650.

FABRICATION, TREATMENT, AND TESTING OF MATERIALS AND STRUCTURES

Effect of the Sapphire-Nitridation Level and Nucleation-Layer Enrichment with Aluminum on the Structural Properties of AlN Layers

T. V. Malin[a]*, D. S. Milakhin[a], V. G. Mansurov[a], Yu. G. Galitsyn[a], A. S. Kozhuhov[a], V. V. Ratnikov[b], A. N. Smirnov[b], V. Yu. Davydov[b], and K. S. Zhuravlev[a, c]

[a] *Rzhanov Institute of Semiconductor Physics, Russian Academy of Sciences, Siberian Branch, 630090 Russia*
[b] *Ioffe Institute, St. Petersburg, 194021 Russia*
[c] *Novosibirsk State University, Novosibirsk, 630090 Russia*
**e-mail: mal-tv@isp.nsc.ru*

Submitted April 4, 2017; accepted for publication April 10, 2017

Abstract—The effect of atomic aluminum deposited onto sapphire substrates with different nitridation levels on the quality of AlN layers grown by ammonia molecular-beam epitaxy is investigated. The nitridation of sapphire with the formation of ~1 monolayer of AlN is shown to ensure the growth of layers with a smoother surface and better crystal quality than in the case of the formation of a nitrided AlN layer with a thickness of ~2 monolayers. It is demonstrated that the change in the duration of exposure of nitrided substrates to the atomic aluminum flux does not significantly affect the parameters of subsequent AlN layers.

DOI: 10.1134/S1063782618060143

1. INTRODUCTION

Group-III element nitrides are direct-gap materials with a band gap from 3.4 to 6.2 eV [1], which are characterized by a high thermal conductivity and therefore are considered to be promising candidates for optoelectronic and high-current electronic applications. Device heterostructures based on Group-III nitrides are formed by epitaxial techniques, including metalorganic chemical vapor deposition (MOCVD), ammonia molecular-beam epitaxy (NH3-MBE), and plasma-assisted molecular-beam epitaxy (PA MBE). At present, the most widely used of the available substrate material for the epitaxial growth of Group-III nitrides is sapphire.

The growth of Group-III nitrides on a sapphire substrate involves a number of technological difficulties caused by a pronounced mismatch between the crystal-lattice parameters of sapphire (a_s = 4.76 Å) and the grown AlN/GaN film (a_f = 3.11 Å/3.18 Å), which amounts to $(a_s - a_f)/a_s$ = (53.1–49.7)%, as well as between the thermal-expansion coefficients of sapphire (5.0×10^{-6} K^{-1}) and AlN (2.9×10^{-6} K^{-1}) [2, 3]. During the establishment of epitaxial technologies, a sequence of growth procedures to solve the mismatch problem were developed. A required initial growth stage was the nitridation of sapphire, which consists in exposure of a heated sapphire substrate under ammonia flux [4–14]. In the course of nitridation, an AlN layer with a unit cell turned by 30° relative to the sapphire unit cell forms on the sapphire surface. This AlN layer is located above the hexagonal sapphire quasi-cell with an effective period of 2.75 Å containing three aluminum atoms and three octahedral voids, which reduces the mismatch between sapphire and AlN crystal lattices to 13% [2, 3].

The nitridation process is complex and consists of several stages. According to the data reported in [10], at the beginning of nitridation, AlN nuclei arise on the sapphire surface, which then grow and form a continuous AlN coating. Further nitridation of sapphire leads to an increase in the AlN-layer thickness. As a result, the nitrided layer consists of misoriented AlN crystalline domains and has a developed surface morphology [10]. The kinetics of AlN formation upon nitridation has been intensively investigated using different techniques. In [4–8], the concentration of bound nitrogen was studied by X-ray photoelectron spectroscopy (XPS) and Auger electron spectroscopy (AES). Grandjean et al. [9] used reflection high-energy electron diffraction (RHEED) to detect the AlN reflection intensity and measure the AlN crystal-lattice constant. These investigations showed that AlN formation during nitridation includes two clearly pronounced stages. At first, AlN forms at a high rate; then, the process slows down and becomes saturated. In the case of the rapid formation of AlN on sap-

phire in the course of nitridation, the AlN diffraction spots width decreases [11, 12], which can be related to an increase in the lateral sizes of newly formed AlN phase nuclei. After that, nitridation of the underlying sapphire layers occurs and the nitridation rate decreases due to the diffusion of active nitrogen deeper into sapphire through the newly formed AlN single layer.

The AlN formation rate depends on the nitridation conditions. Uchida et al. [4] showed that, at an ammonia flux of 1400 sccm and a sapphire substrate temperature of 1050°C, the rapid stage of nitridation in a MOCVD facility changes to the slow stage 3 min after the beginning of the process [4]. According to the data from [9], at a substrate temperature of 850°C in an ammonia flux of 20 sccm in an NH3-MBE facility, the process saturates 10 min from the beginning of nitridation. We established that during NH3-MBE, the rapid nitridation time varies from 120 s to 60 min upon a substrate temperature variation from 500 to 1000°C and an ammonia pressure change in the range from 12.5 to 400 sccm [11, 12]. Heinlein et al. [5] investigated the nitridation process in a PA MBE facility at a substrate temperature of 400°C and found that a continuous AlN layer only forms 300 min after the beginning of nitridation. Dwikusuma et al. [7] did not observe nitridation saturation upon the exposure of a sapphire substrate heated to 700°C to a nitrogen-ion flux. Since the rate of nitridation stages depends on the nitridation conditions, the crystal quality of the subsequent Group-III nitride layers depends on the substrate nitridation conditions, i.e., temperature, ammonia pressure, and time of exposure in ammonia [4, 9, 13–17].

It is important to determine the nitridation stage at which epitaxial growth can be started. Although the nitridation conditions change the process rate, the character of the process is similar for different conditions; therefore, of great importance is the degree of process completeness [11, 12]. Usually, researchers focus on the nitridation time. It was demonstrated in [4–9] that there exists some optimal nitridation time, while short or too long nitridation times result in degradation of the subsequent epitaxial layer quality. Since time is not the only parameter determining the nitridation rate, solving this problem requires choosing a criterion for the degree of nitridation completeness (formation of a continuous AlN layer). In this study, we propose the use of the AlN(01) diffraction spot intensity in the $[12\bar{1}0]$ direction upon nitridation as such a criterion.

Ultrathin AlN layers formed upon nitridation can be graphene-like and nonpolar (see [18, 19]). To repeatedly obtain the metal polarity, the growth of subsequent layers is usually started at a metal excess. To attain the conditions for enrichment with aluminum, Yoshikawa et al. [20] proposed the growth of AlN layers on top of nitrided sapphire by epitaxy with the enhanced migration of atoms [20]. Liu et al. [21] reported the formation of metal polarity by the deposition of a low-temperature (600°C) thin (30-nm) AlN (LT AlN) layer on top of nitrided sapphire; in this case, the growth of Group-III nitrides without LT AlN deposition leads to the formation of layers with nitrogen polarity. Ohta et al. [22] showed the effective suppression of N-polarity inversion domains with the use of an added AlN layer grown under the conditions of enrichment with Al; when a GaN layer grown in the Ga-rich conditions, this effect was not observed. Davidsson et al. [23] studied the effect of the Al/N flux ratio on the polarity of GaN layers formed by the PA MBE technique and established that the conditions of enrichment with Al, when the Al/N flux ratio is Al/N = 0.6 and the AlN nucleation-layer thickness is 3 nm, are optimal for obtaining high-quality metal-polarity layers. In [24, 25], the possibility of attaining metal polarity by the deposition of two aluminum monolayers by PA-MBE was demonstrated. The deposition of more than two aluminum monolayers from trimethylaluminum onto nitrided sapphire substrate before growing a GaN buffer layer by the MOCVD technique was used in [26] to change the growing layer polarity. As the deposition time increases, the *N* polarity of the investigated GaN layer changed to mixed polarity and, at a deposition time of more than 5 s, a metal-polarity GaN layer formed [26]. Thus, we can conclude that AlN growth under the Al-rich conditions allows metal-polarity layers to be formed. However, data on the thickness and growth conditions of the AlN nucleation layer demonstrating metal polarity are very controversial. In addition, no researchers have thus far considered the effect of the conditions of AlN nucleation-layer formation at different levels of nitridation completeness.

In this study, we investigate the effect of excess aluminum deposited onto a sapphire substrate nitrided to different degrees of completeness on the quality of AlN layers.

2. EXPERIMENTAL

The investigated AlN samples were grown using a Riber CBE-32(N) facility. The aluminum sources were standard effusion cells and the active nitrogen source was ammonia. The ammonia flux in the chamber was controlled with a mass-flux controller operating in the range of 0–400 sccm. The substrates were heated by the absorption of the infra-red radiation of a heater; for this purpose, the sapphire substrate's backside was coated with a 0.4-μm-thick molybdenum layer. Before the experiment, the substrates were cleaned by annealing in a loading chamber at a temperature of 900°C for 1 h. Then, sapphire was exposed under ammonia flux and the nitrided sapphire substrate was coated with aluminum. At the final stage, a 1-μm-thick AlN layer was grown in an ammonia flux

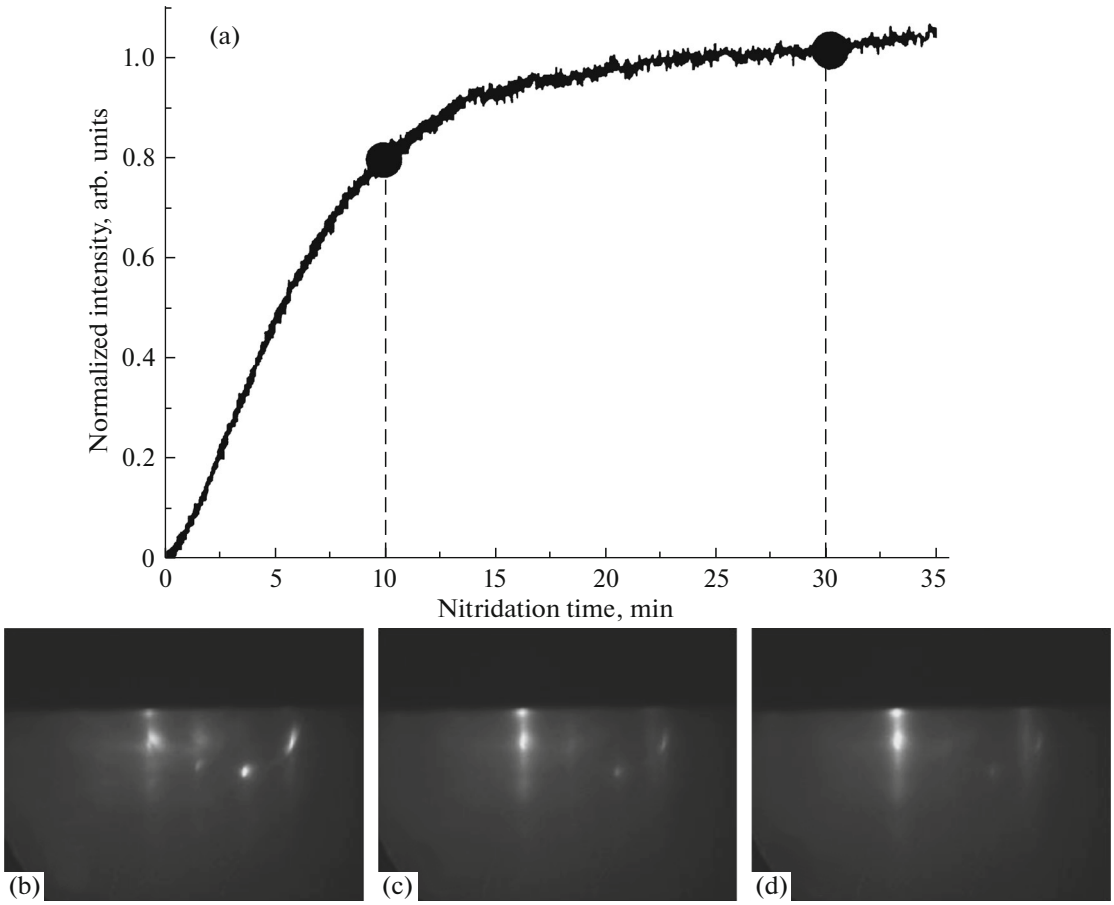

Fig. 1. (a) Kinetic curve of the nitridation process at a temperature of 840°C in an ammonia flux of 25 sccm and diffraction patterns of (b) the initial sapphire surface and sapphire after nitridation for (c) 10 and (d) 30 min.

of 15 sccm at a substrate temperature of 940°C and a rate of 0.3 μm/h.

The morphology of the obtained AlN layers was studied by reflection high-energy electron diffraction (RHEED) and atomic force microscopy (AFM). The crystal quality of the films was estimated by X-ray diffraction (XRD) and Raman scattering. X-ray structure investigations were carried out using a three-crystal X-ray spectrometer. Raman spectra were detected in the backscattering mode at room temperature using a Horiba Jobin–Yvon T64000 spectrometer. The excitation source was a Nd:YAG laser with a wavelength of 532 nm.

2.1. Sapphire Nitridation

The kinetic curve of the nitridation process at a temperature of 840°C in an ammonia flux of 25 sccm is shown in Fig. 1a. The curve shows the variation in the intensity of the reflection from the AlN phase newly formed on the sapphire surface. It can be seen from Fig. 1a that AlN formation on the sapphire surface first occurs at a high rate, then decreases, and becomes saturated ~30 min after the beginning of nitridation. Figures 1b–1d show the diffraction patterns of the initial sapphire surface and sapphire after nitridation for 10 and 30 min, which correspond approximately to the middle and end of the rapid nitridation portion. The diffraction pattern obtained after 10-min nitridation (Fig. 1c) shows reflections from the sapphire surface in the [11–20] direction and a weak reflection from newly formed AlN. The low intensity of the AlN reflection is indicative of the small degree of surface coating and a small AlN layer thickness. In the diffraction pattern obtained after 30-min nitridation (Fig. 1d), the reflection from the AlN crystalline phase is much brighter and the intensity of reflections from sapphire is lower. Comparison of these diffraction patterns with the patterns from [27] (see Figs. 2 and 4 from [27]), where the nitrided layer thickness was measured by the XRD technique, allows us to conclude that the thickness of the nitrided layer is ~2 Å (~1 monolayer, 1 ML) and 5–7 Å (~2 ML) after the 10- and 30-min nitridation, respectively.

The distance between the neighboring AlN (00) and (01) streaks changes with time, which is indicative of the AlN lattice-constant variation. Figure 2 shows

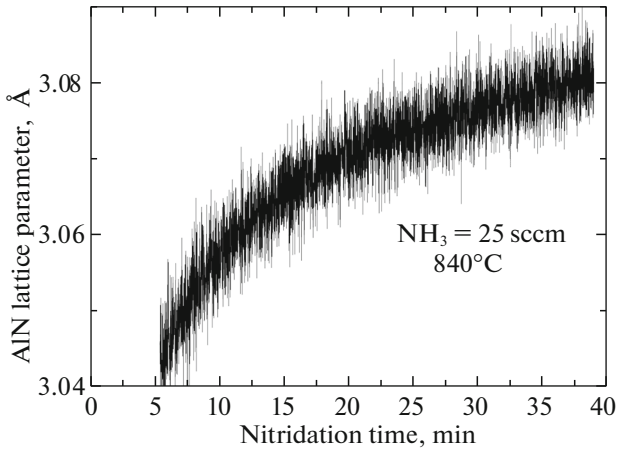

Fig. 2. Variation in the AlN crystal-lattice parameter during nitridation at 840°C in a flux of NH_3 = 25 sccm.

the dependence of the AlN crystal-lattice parameter *a* on the nitridation time. It can be seen that the AlN crystal-lattice parameter changes from 3.01 to 3.08 Å. It is worth noting that we failed to accurately measure the AlN crystal-lattice parameter in the very beginning of the nitridation process, since the signal from AlN is insufficient to precisely determine its position. Nevertheless, the obtained AlN crystal-lattice constants do not coincide with the values reported in [9], where it was shown that during nitridation the AlN crystal-lattice parameter changes from 2.75 Å (the sapphire quasi-cell parameter) to 3.11 Å (the bulk AlN lattice parameter). It is possible that the lattice parameter of newly formed AlN is 3.01 Å rather than 2.75 Å; then, the mismatch between the crystal-lattice parameters of the surface sapphire cell and AlN is merely (3–4)%. We note that 3.01 Å is a important value revealed by AFM for the pure Al_2O_3 sapphire surface [28].

To study the effect of sapphire nitridation on the surface morphology and crystal quality of the AlN layers, we grew the layers on the initial (non-nitrided) and nitrided (at different levels) sapphire surfaces. The different nitridation levels (1 ML and 2 ML) are shown by dots on the nitridation kinetic curve (Fig. 1a). The AlN layer grown on the non-nitrided AlN substrate has a polycrystalline structure (Fig. 3a), which is different from the results obtained in [4, 13–16], where crystal layers were formed on non-nitrided sapphire. The difference can be attributed to unintentional sapphire nitridation at the instant of opening the ammonia flux under MOCVD conditions. This can occur at temperatures of over 950°C in ammonia fluxes of over 100 sccm, when the nitridation rate is very high [16].

2.2. Deposition of Aluminum

At the next stage, we studied the effect of aluminum deposition on the crystal quality of subsequent AlN layers. For this purpose, we varied the time of exposure of the sapphire substrates for a fixed atomic aluminum flux that was equivalent to a pressure of 1.0×10^{-7} Torr at a switched-off ammonia flux. The deposition of aluminum for 30 s corresponds to sapphire surface coating with Al with a thickness of about 2 ML and 300-s deposition corresponds to coating with a thickness of 20 ML. This allowed us to form a nucleation layer at an Al excess at Al/N ratios of 2/1 and 20/1, respectively. The deposition of aluminum was followed by AlN layer growth, which started from the simultaneous opening of an ammonia injector and aluminum source shutter at an Al/N ratio of 1/10. Table 1 gives the times of nitridation and exposure of a nitrided substrate in an aluminum flux. Hereinafter, the samples are designated using a slash dividing the nitridation time (min) and time of exposure to the aluminum flux (s). Two samples, 10N/0Al and 30N/0Al, were grown without exposure of the nitrided substrate to the aluminum flux.

3. RESULTS OF INVESTIGATIONS OF THE AlN LAYERS AND DISCUSSION

The surface morphology of the obtained AlN layers was estimated by the RHEED and AFM techniques. Figure 3 shows the diffraction patterns of the surface of

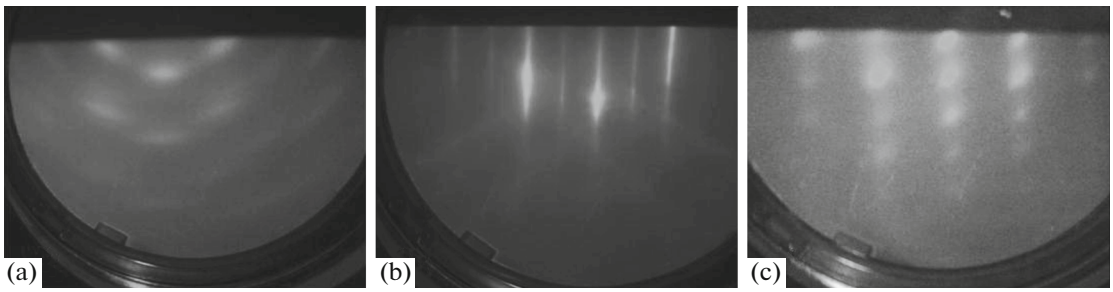

Fig. 3. Diffraction patterns of the AlN layer surface in the [11–20] direction: (a) a sample grown on a non-nitrided sapphire substrate; (b) samples 10N/0Al, 10N/30Al, and 10N/300Al; and (c) samples 30N/0Al, 30N/30Al, and 30N/300Al. The nitridation temperature is 500°C and the NH_3 flux is 15 sccm.

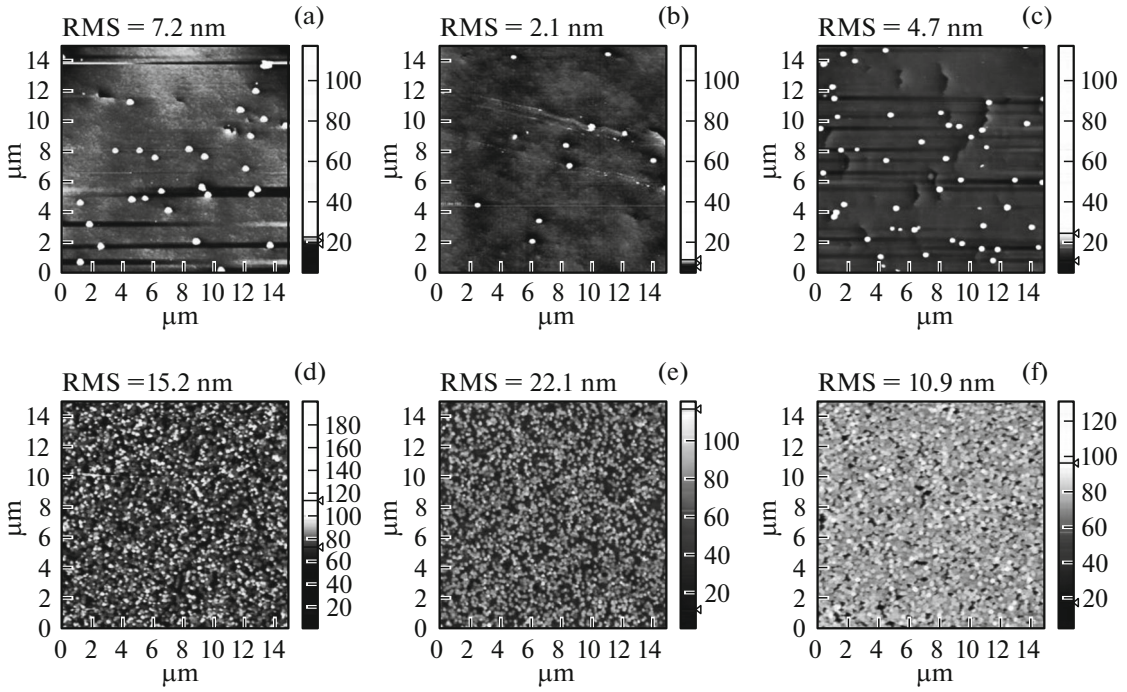

Fig. 4. AFM images (15 × 15 μm^{-2}) of the investigated AlN layers. Samples: (a) 10N/0Al, (b) 10N/30Al, (c) 10N/300Al, (d) 30N/0Al, (e) 30N/30Al, and (f) 30N/300Al.

the AlN samples obtained at a temperature of 500°C in an ammonia flux of 15 sccm. The diffraction patterns of samples 10N/0Al, 10N/30Al, and 10N/300Al contain narrow reflections typical of a smooth surface (two-dimensional diffraction pattern). The pronounced reflections of the (2 × 2) surface reconstruction are indicative of the metal polarity of AlN layers [29–31]. The change in the time of exposure of the layers to the aluminum flux in no way do not affect the diffraction patterns. The diffraction patterns of samples 30N/0Al, 30N/30Al, and 30N/300Al have traces of transmission diffraction (three-dimensional diffraction pattern) typical of a surface with a developed morphology and contain no reconstruction reflections. The developed surface pattern can result from a great number of misoriented or inclined AlN domains and the presence of a great number of inversion domains, which grow faster than columns with metal polarity [32]. The absence of the (2 × 2) surface reconstruction is also related to inversion domains since the surface of layers with nitrogen polarity does not form the (2 × 2) reconstruction at 500°C in an ammonia flux [29–31]. The increased width of reflections from the surface of AlN samples 30N/0Al, 30N/30Al, and 30N/300Al indicates the high degree of surface granularity. The variation of surface exposition in the aluminum flux did not affect the diffraction pattern.

The RHEED data on the surface morphology are consistent with the AFM data. Figure 4 shows AFM images of an AlN layer surface of 15 × 15 μm^{-2} in size. The surface morphology of all the samples with a nitrided layer thickness of 1 ML is smooth. The root-mean-square (RMS) surface roughness is small (2.1–7.2 nm) and the inversion domain density is relatively low (0.07–0.4 μm^{-2}). The lowest density of inversion domains is observed in sample 10N/30Al. In addition, this sample has the lowest roughness: RMS = 2.1 nm. The surface of AlN samples with a nitrided layer thickness of 2 ML has, in contrast, the high density of inversion domains (17–25 μm^{-2}) with a height of about 70–90 nm and features a developed morphology; in this case, RMS = 10.9–22.1 nm.

Sample 30N/30Al has the largest roughness, RMS = 22.1 nm; however, it is characterized by the lowest density of inversion domains (~18 μm^{-2}). This feature can be caused by the higher inversion-domain

Table 1. Designations of AlN samples with different nitridation and nucleation times

Duration of atomic aluminum deposition		0 s	30 s	300 s
Nitridation time	10 min	10N/0Al	10N/30Al	10N/300Al
	30 min	30N/0Al	30N/30Al	30N/300Al

Table 2. XRD data on the AlN layers

Duration of atomic aluminum deposition time			0 s	30 s	300 s
Nitridation time	10 min	R, m	+31.9	+27.3	+32.7
		σ_a, GPa	+0.53	+0.62	+0.52
		FWHM (0002), arcsec	505	422	588
		ρ_{screw}, 10^9 cm^{-2}	0.55	0.39	0.75
		FWHM ($10\bar{1}5$), arcsec	991	874	1010
		ρ_{edge}, 10^9 cm^{-2}	4.91	3.82	5.1
	30 min	R, m	+75.0	+67.0	+34.7
		σ_a, GPa	+0.23	+0.25	+0.59
		FWHM(0002), arcsec	1029	656	803
		ρ_{screw}, 10^9 cm^{-2}	2.3	0.94	1.4
		FWHM ($10\bar{1}5$), arcsec	1507	832	961
		ρ_{edge}, 10^9 cm^{-2}	11.3	3.5	4.6

density in samples 30N/0Al and 30N/300A. Closely packed inversion domains decrease the calculated RMS value, since their surface has no dips up to AlN surface regions with metal polarity. The presented data show that the optimal time of exposure to the atomic Al flux for the samples with a nitrided layer thickness of 2 ML is 30 s. Although the RMS value of this sample is larger, it has the lowest inversion domain density (17 μm^{-2}).

The structural properties of AlN layers were studied by XRD and Raman scattering methods. The crystal quality of the layers was estimated from the measured full width at half-maximum (FWHM) of X-ray reflections and FWHM values of the E_2 band (high) in the Raman scattering spectra. We measured the FWHM of symmetric reflection 0002 corresponding to the micro-misorientations of the {0001} planes caused mainly by defects of vertical screw dislocations with density ρ_{screw} and the half-width of the skew-geometry reflection 10-15; this density is sensitive to displacements due to, in particular, the presence of vertical edge and mixed dislocations with density ρ_{edge}. The dislocation densities were calculated using the formula for randomly distributed dislocations [33]. The measured XRD data are listed in Table 2. It can be seen from Table 2 that the smallest FWHM values of the symmetric and skew symmetric reflections and, consequently, the calculated densities of vertical screw and mixed dislocations correspond to layers subjected to 30-s exposure to an Al flux at both nitridation times. The rocking curves for sample 30N/300Al are non-symmetric; therefore, we failed to determine the FWHM values for this sample. Such a situation is typical of the layers with two pronounced types of misorientation of the growing domains. According to the XRD data, the smallest FWHM values for the symmetric and skew symmetric reflections characterize sample 10N/30Al. The Raman scattering spectra are shown in Fig. 5. The highest-quality crystal structure is observed in samples 30N/300Al, 30N/30Al, and 10N/30Al, for which the FWHM value of the E_2 symmetry band (high) is within 4.1–4.3 cm^{-1} (Table 3). In addition, it is worth noting that the spectra of samples 30N/0Al and 30N/30Al include an additional feature near 613–614 cm^{-1}, which can be related to the phonon symmetry line A_1 (TO) forbidden in this scattering geometry. The occurrence of this line is, most likely, indicative of a slight deviation of the hexagonal axis of the AlN layers from the sample surface normal in the direction similar to [10—12, 34].

In addition, we used the XRD technique to measure the bending radius R, which brings information about homogeneous lateral biaxial compressive

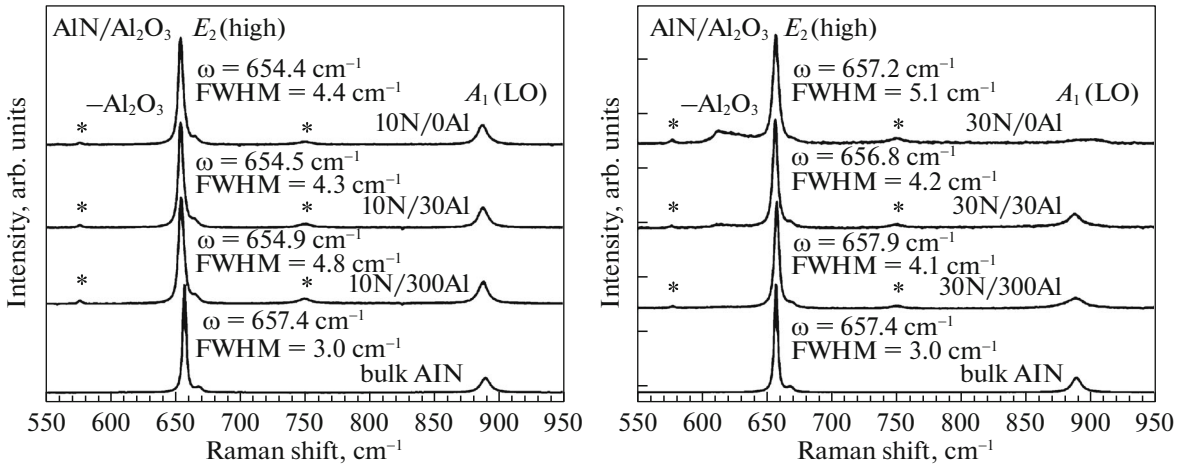

Fig. 5. Polarized Raman scattering spectra of the investigated AlN layers. T = 300 K, excitation at a wavelength of 532 nm, and the scattering geometry $z(xx)z$ (z coincides with the AlN layer growth direction).

Table 3. Raman spectroscopy data for the samples

Duration of atomic aluminum deposition time			0 s	30 s	300 s
Nitridation time	10 min	$\Delta\omega$, cm^{-1}	−3.0	−2.9	−2.5
		σ_a, GPa	+0.48	+0.46	+0.40
		FWHM E_2 (high), cm^{-1}	4.4	4.3	4.8
	30 min	$\Delta\omega$, cm^{-1}	−0.2	−0.6	+0.5
		σ_a, GPa	+0.03	+0.1	−0.08
		FWHM E_2 (high), cm^{-1}	5.1	4.2	4.1

stresses σ_a ($R < 0$) or tensile stresses ($R > 0$). The σ_a values were calculated using the Stoney formula [35]; bending of the initial sapphire substrates was taken into account in calculations. All the samples with a nitrided-layer thickness of 1 ML, regardless of the atomic Al deposition time, were concave from the layer side with a uniform bending radius of $R \approx -30$ m, which is indicative of the presence of tensile stresses in the layers and a σ_a value of about +0.55 GPa on average. The tensile stresses in the films with a nitrided-layer thickness of 2 ML are twice as low as in the samples with a nitrided-layer thickness of 1 ML, except for sample 30N/300Al exposed to the Al flux for 5 min, for which σ_a = +0.59 GPa. Similar results were obtained by the Raman scattering technique (Table 3). The quantity $\Delta\omega$ in Table 3 is the difference between the measured frequency of oscillations of E_2 symmetry phonons (high) and a value of 657.4 cm^{-1} for unstrained AlN [36]. The negative frequency difference means that the investigated AlN films are expanded. The stresses in the AlN layer plane were determined using the formula $\sigma_a = \Delta\omega/K$, where $K = -6.3$ [36]. All the samples with a nitrided-layer thickness of ~1 ML, regardless of the atomic aluminum deposition time, have a σ_a value of about +0.45 GPa on average. The tensile stresses in the films with a nitrided-layer thickness of ~2 ML are almost lacking. In sample 30N/300Al exposed to the Al flux for 5 min, the stresses are compressive and σ_a = +0.08 GPa. The observed trends in stress variation in the AlN layers established by XRD and Raman scattering are in good agreement.

The observation of tensile stresses in the AlN layers on Al_2O_3 is a nontrivial result, since the differences between the bulk lattice parameters of Al_2O_3 and AlN should lead to the occurrence of compressive stresses in the AlN layers. The presence of tensile stresses in the AlN layers can be attributed to the mechanism proposed in [37], assuming this mechanism prevails over the compressive stresses induced by the lattice parameter of the substrate. In [37], Hoffman considered the formation of internal stresses introduced into an AlN layer during growth upon the joining of individual islands. A weakening or absence of tensile stresses in AlN layers with a nitrided-layer thickness of ~2 ML can result from the compensation of tensile stresses arising during the intergrowth of AlN by compressive stresses caused by a difference between the AlN and Al_2O_3 lattice parameters.

4. CONCLUSIONS

It is established that the nitridation of sapphire with the formation of ~1 ML of AlN on its surface ensures the subsequent growth of AlN layers with a smoother surface and better crystal quality as compared with the nitridation of sapphire with the formation of a thicker (~2 ML) AlN layer. This can be related to the fact that an increase in the nitrided-layer thickness leads to the formation of a great number of deflected AlN nuclei and to an increase in the number of inversion domains. Exposure of the nitrided substrates to an atomic aluminum flux only affects the structural parameters of the AlN layers. At an exposure time corresponding to coating of the nitrided sapphire surface with ~2 ML of atomic aluminum, the FWHM values of the X-ray reflections decrease as compared with the samples without aluminum; a further increase in the exposure time results in degradation of the crystal quality of the films.

Thus, nitridation with the formation of ~1 ML of AlN crystalline phase with AlN nucleation upon exposure to the atomic Al flux leading to the formation of an about 2-ML atomic Al coating on the nitrided sapphire surface makes it possible to grow AlN layers with the best parameters by ammonia MBE.

ACKNOWLEDGMENTS

This study was supported by the Russian Foundation for Basic Research, project nos. 16-32-00773, 17-02-00947, and 16-02-00702.

REFERENCES

1. S. Strite and H. Morkoc, J. Vac. Sci. Technol. **10**, 1237 (1992).
2. T. Yamaguchi, T. Araki, Y. Saito, K. Kano, H. Kanazawa, Y. Nanishi, N. Teraguchi, and A. Suzuki, J. Cryst. Growth **237–239**, 993 (1994).
3. K. Masu, Y. Nakamura, T. Yamazaki, T. Shibata, M. Takahashi, and K. Tsubouchi, Jpn. J. Appl. Phys. **34** (6B), 760 (1995).
4. K. Uchida, A. Watanabe, F. Yano, M. Kouguchi, T. Tanaka, and S. Minagawa, J. Appl. Phys. **79**, 3487 (1996).
5. Ch. Heinlein, J. Grepstad, T. Berge, and H. Riechert, Appl. Phys. Lett. **71**, 341 (1997).

6. A. Georgakilas, S. Mikroulis, V. Cimalla, M. Zervos, A. Kostopoulos, Ph. Komninou, Th. Kehagias, and Th. Karakostas, Phys. Status Solidi A **188**, 567 (2001).
7. F. Dwikusuma and T. F. Kuech, J. Appl. Phys. **94**, 5656 (2003).
8. B. Agnarsson, M. Göthelid, S. Olafsson, H. P. Gislason, and U. O. Karlsson, J. Appl. Phys. **101**, 013519 (2007).
9. N. Grandjean, J. Massies, and M. Leroux, J. Appl. Phys. **69**, 2071 (1996).
10. M. Yeadon, M. T. Marshall, F. Hamdani, S. Pekin, H. Morkoc, and J. Murray Gibson, J. Appl. Phys. **83**, 2847 (1998).
11. T. Malin, V. Mansurov, Y. Galitsyn, and K. Zhuravlev, Phys. Status Solidi C **11**, 613 (2014).
12. T. Malin, V. Mansurov, Y. Galitsyn, and K. Zhuravlev, Phys. Status Solidi C **12**, 443 (2015).
13. Y. Wu, A. Hanlon, J. F. Kaeding, R. Sharma, P. T. Fini, S. Nakamura, and J. S. Speck, Appl. Phys. Lett. **84**, 912 (2004).
14. W.-G. Hu, Ch.-M. Jiao, H.-Y. Wei, P.-F. Zhang, T. T. Kang, R.-Q. Zhang, and X.-L. Liu, Chin. Phys. Lett. **25**, 4364 (2008).
15. K. S. Kim, K. Y. Lim, and H. J. Lee, Semicond. Sci. Technol. **14**, 557 (1999).
16. L.-C. Le, D.-G. Zhao, L.-L. Wu, Y. Deng, D.-S. Jiang, J.-J. Zhu, Z.-S. Liu, H. Wang, S.-M. Zhang, B.-S. Zhang, and H. Yang, Chin. Phys. B **20**, 127306 (2011).
17. W. Kim, M. Yeadon, A. E. Botchkarev, S. N. Mohammad, J. M. Gibson, and H. Morkoc, J. Vac. Sci. Technol. B **15**, 921 (1997).
18. C. L. Freeman, F. Claeyssens, and N. L. Allan, Phys. Rev. Lett. **96**, 066102 (2006).
19. C. J. F. Solano, A. Costales, E. Francisco, A. M. Pendas, M. A. Blanco, K.-C. Lau, H. He, and R. Pandey, J. Phys. Chem. C **112**, 6667 (2008).
20. A. Yoshikawa and K. Takahashi, Phys. Status Solidi A **188**, 625 (2001).
21. F. Liu, R. Collazo, S. Mita, Z. Sitar, G. Duscher, and S. J. Pennycook, J. Appl. Phys. Lett. **91**, 203115 (2007).
22. J. Ohta, H. Fujioka, M. Oshima, K. Fujiwara, and A. Ishii, Appl. Phys. Lett. **83**, 3075 (2003).
23. S. K. Davidsson, J. F. Falth, X. Y. Liu, H. Zirath, and T. G. Andersson, J. Appl. Phys. **98**, 016109 (2005).
24. K. Xu, N. Yano, A. W. Jia, A. Yoshikawa, and K. Takahashi, J. Cryst. Growth **237–239**, 1003 (2002).
25. Y. S. Park, H. S. Lee, J. H. Na, H. J. Kim, S. M. Si, H. M. Kim, and J. E. Oh, J. Appl. Phys. **94**, 800 (2003).
26. D. H. Lim, K. Xu, S. Arima, A. Yoshikawa, and K. Takahashi, J. Appl. Phys. **91**, 6461 (2002).
27. Y. Wang, A. S. Ozcan, G. Ozaydin, K. F. Ludwig, Jr., A. Bhattacharyya, Th. D. Moustakas, H. Zhou, R. L. Headrick, and D. P. Siddons, Phys. Rev. B **74**, 235304 (2006).
28. J. V. Lauritsen, M. C. R. Jensen, K. Venkataramani, B. Hinnemann, S. Helveg, B. S. Clausen, and F. Besenbacher, Phys. Rev. Lett. **103**, 076103 (2009).
29. A. R. Smith, R. M. Feenstra, D. W. Greve, J. Neugebauer, and J. E. Nortrhrup, Phys. Rev. Lett. **79**, 3934 (1997).
30. A. R. Smith, R. M. Feenstra, D. W. Greve, M.-S. Shin, M. Skowronski, J. Neugebauer, and J. E. Nortrhrup, Surf. Sci. **423**, 70 (1999).
31. N. Kumagai, K. Akiyama, R. Togashi, H. Murakami, M. Takeuchi, T. Kinoshita, K. Takada, Y. Aoyagi, and A. Koukitu, J. Cryst. Growth **305**, 366 (2007).
32. O. Ambacher, J. Phys. D **31**, 2653 (1998).
33. C. G. Dunn and E. F. Koch, Acta Metall. **5**, 548 (1957).
34. L. Filippidis, H. Siegle, A. Hoffmann, C. Thomsen, K. Karch, and F. Bechstedt, Phys. Status Solidi B **198**, 621 (1996).
35. G. G. Stoney, Proc. R. Soc. London **82** (553), 172 (1909).
36. T. Prokofyeva, M. Seon, J. Vanbuskirk, and M. Holtz, Phys. Rev. B **63**, 125313 (2001).
37. R. W. Hoffman, Thin Solid Films **34**, 185 (1976).

Translated by E. Bondareva